THE ACCURACY AND INFORMATION CONTENT OF SATELLITE ATMOSPHERIC VERTICAL PROFILE MEASUREMENTS

G. A. Kelly*

European Centre for Medium Range Weather Forecasts,

Reading, Berkshire, United Kingdom

1. INTRODUCTION

The aims of this paper are to describe the characteristics of the operational NOAA satellites vertical sounding system, briefly summerise the radiative theory, describe some earlier work of Dr. W. Smith using data from the NIMBUS satellite series relating to the effect of using a statistical and a direct solution methods, and present comparisons of current satellite derived temperature and humidity profile with radiosonde measurements.

---

* ECMWF visiting Scientist on leave from Bureau of Meteorology Research Centre (BMRC), 150 Lonsdale St., Melbourne, Australia.

2. SPACECRAFT SOUNDING SYSTEM

The TIROS-N NOAA A-G series of satellites began operating in October 1978. These satellites are high-quality observation platforms supplying large amounts of data describing the Earth's surface and enveloping atmosphere. The TIROS-N Operational Vertical Sounder (TOVS) (Smith, et al. (1979)) instrument packages on board all these satellites allow vertical temperature and moisture structures (soundings) to be calculated between the surface and the stratopause. Ideally two satellites are operational and are in sun-synchronous polar orbit at any one time. This implies a full global coverage by these satellites every 6 hours.

The TOVS package consists of three radiance measuring instruments: the High-resolution Infrared Radiation Sounder (HIRS), sampling at 20 infrared frequencies, the Microwave Sounding Unit (MSU), sampling at 4 microwave frequencies, and the Stratospheric Sounding Unit (SSU), sampling at three additional infrared frequencies. Typical scan patterns of the HIRS and MSU instruments across the suborbital track are shown in Fig. 1. The HIRS instrument resolves a mean area 30 km in diameter at the sub-satellite point, whereas the MSU resolves a circular area of 110 km in diameter. There are 56 fields of view (fov) within each scan line width of approximately 2,250 km for the HIRS instrument. Only 11 fovs are completed in every MSU scan line in the time the HIRS instrument takes for 5 scan lines or 280 fovs. For both instruments, the fov "footprints" become elliptical and enlarge as the fov location is removed further from the sub-satellite point.

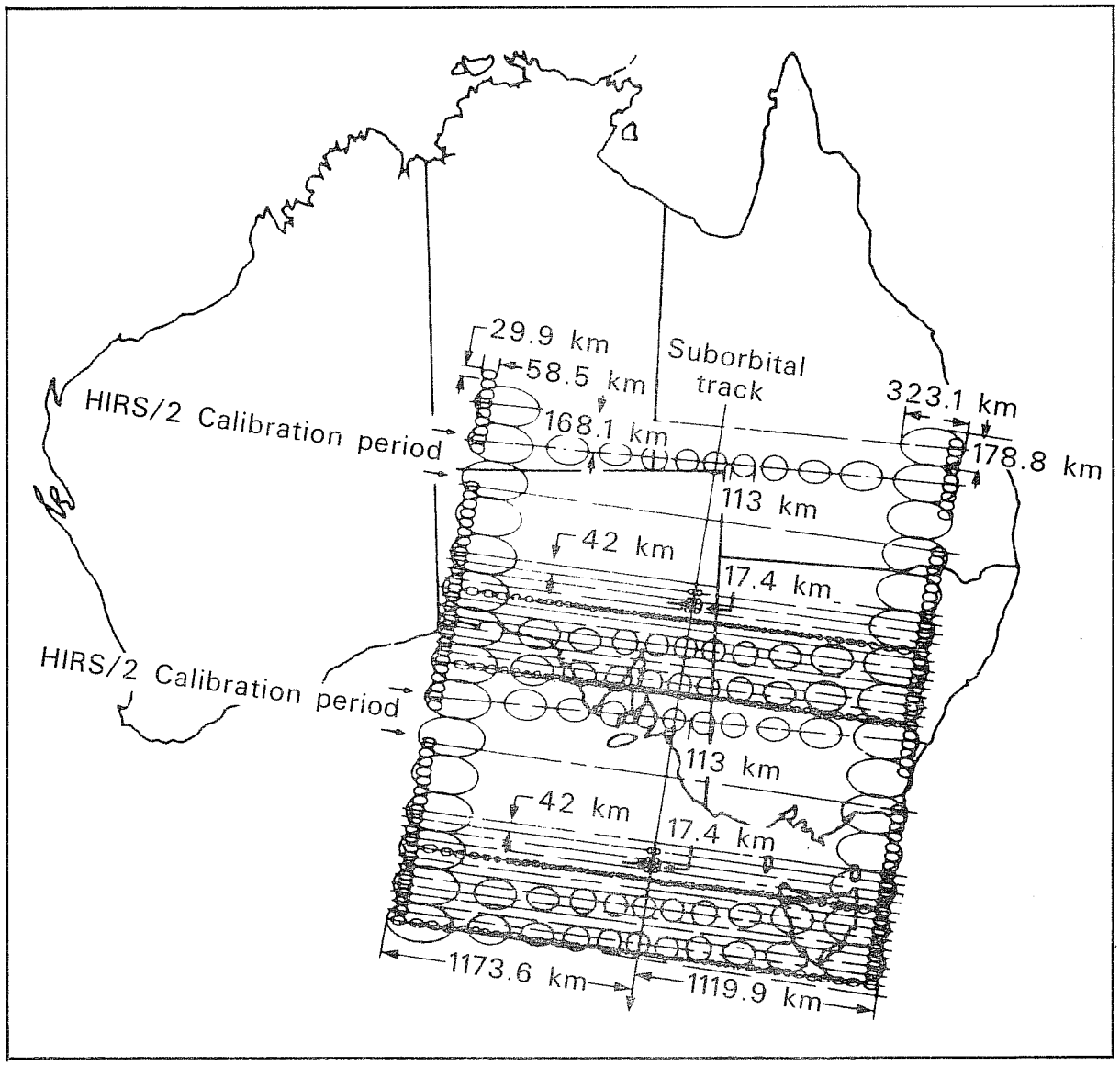

Fig. 1: Typical TOVS orbit showing the resolution of the HIRS and MSU instruments. The orbital direction is from the top right to the bottom left of the figure.

In order to reduce the processing so that the output can be transmitted via the GTS the HIRS and MSU data are processed in boxes. Presently these boxes are 7 by 9 arrays of HIRS scan spots and associated MSU data. The processing then computes the cloud free radiances in the boxes. This often has been referred to as the derivation of "clear-column" radiances. A complex objective analysis scheme is used to detect if there are truly clear scan spots within the array. If there are at least four, they are averaged to produce a radiance set for a "clear" sounding which is located at the centroid of the individual clear scan spots. If there are not a minimum of four clear spots, the array is processed to determine if there are enough partly cloudy areas which can pass a complex series of quality tests to be acceptable for further processing as a "partly cloudy" sounding. Finally, those arrays which fail these tests are classified as "cloudy". In the latter cases, the MSU channels and the four channels of HIRS which sense radiation from the highest part of the atmospheric column, those presumed not to be contaminated by cloud, are compiled for subsequent processing in the retrieval module as "cloudy" soundings. The use of a 7 by 9 array of HIRS fields of view gives a nominal horizontal resolution of the resulting soundings of about 250 km.

3. THEORY

3.1. Radiative Transfer Equation

The physical principal governing the temperature profile measurements is the same for all of these sensors. The temperature structure of the atmosphere is inferred from measurements of the earth's radiance in an absorption band due to a gaseous constituent whose concentration is uniform. (The 4.3μm CO_2, 15μm CO_2, and 5mm O_2 bands are used for the temperature profile sensing. Table 1 shows the TOVS sounding channels characteristics.) The instruments are designed to measure the radiance of different frequencies or wavelengths within one or more of these bands. By varying the frequency, one varies the level of the atmosphere from which the measured radiation originates. For example, absorption is most intense at the center of the band; consequently, this radiation emanates from only the very top of the atmosphere because of the strong attenuation at lower levels. On the other hand, radiation arising from the lowest regions of the atmosphere can be measured at those frequencies far from the band center which are characterized by little absorption. Radiation received from intermediate levels is measured at frequencies associated with moderate absorption.

The outgoing radiance from earth measured by any channel of TOVS is related to the atmosphere's temperature and absorbing gas structure by the radiative transfer equation

Table 1

Characteristics of TOVS sounding channels

HIRS Channel number	Channel central wavenumber	Central wavelength (μm)	Principal absorbing constituents	Level of peak energy contribution	Purpose of the radiance observation
1	668	15.00	CO_2	30 mb	*Temperature sounding.* The 15-μm band channels provide better sensitivity to the temperature of relatively cold regions of the atmosphere than can be achieved with the 4.3-μm band channels. Radiances in Channels 5, 6, and 7 are also used to calculate the heights and amounts of cloud within the HIRS field of view.
2	679	14.70	CO_2	60 mb	
3	691	14.50	CO_2	100 mb	
4	704	14.20	CO_2	400 mb	
5	716	14.00	CO_2	600 mb	
6	732	13.70	CO_2/H_2O	800 mb	
7	748	13.40	CO_2/H_2O	900 mb	
8	898	11.10	Window	Surface	*Surface temperature* and cloud detection.
9	1 028	9.70	O_3	25 mb	*Total ozone* concentration.
10	1 217	8.30	H_2O	900 mb	*Water vapor sounding.* Provides water vapor corrections for CO_2 and window channels. The 6.7-μm channel is also used to detect thin cirrus cloud.
11	1 364	7.30	H_2O	700 mb	
12	1 484	6.70	H_2O	500 mb	
13	2 190	4.57	N_2O	1 000 mb	*Temperature sounding.* The 4.3-μm band channels provide better sensitivity to the temperature of relatively warm regions of the atmosphere than can be achieved with the 15-μm band channels. Also, the short-wavelength radiances are less sensitive to clouds than those for the 15-μm region.
14	2 213	4.52	N_2O	950 mb	
15	2 240	4.46	CO_2/N_2O	700 mb	
16	2 276	4.40	CO_2/N_2O	400 mb	
17	2 361	4.24	CO_2	5 mb	
18	2 512	4.00	Window	Surface	*Surface temperature.* Much less sensitive to clouds and H_2O than the 11-μm window. Used with 11-μm channel to detect cloud contamination and derive surface temperature under partly cloudy sky conditions. Simultaneous 3.7- and 4.0-μm data enable reflected solar contribution to be eliminated from observations.
19	2 671	3.70	Window	Surface	
20	14 367	0.70	Window	Cloud	*Cloud detection.* Used during the day with 4.0- and 11-μm window channels to define clear fields of view.

MSU	Frequency (GHz)	Principal absorbing constituents	Level of peak energy contribution	Purpose of the radiance observation
1	50.31	Window	Surface	*Surface emissivity* and *cloud attenuation* determination.
2	53.73	O_2	700 mb	*Temperature sounding.* The microwave channels probe through clouds and can be used to alleviate the influence of clouds on the 4.3- and 15-μm sounding channels.
3	54.96	O_2	300 mb	
4	57.95	O_2	90 mb	

SSU	Wavelength (μm)	Principal absorbing constituents	Level of peak energy contribution	Purpose of the radiance observation
1	15.0	CO_2	15.0 mb	*Temperature sounding.* Using CO_2 gas cells and pressure modulation, the SSU observes thermal emissions from the stratosphere.
2	15.0	CO_2	4.0 mb	
3	15.0	CO_2	1.5 mb	

$$R(\nu) = B_\nu[T(Po)]\,\tau_\nu(Po) - \int_o^{Po} B_\nu[T(p)]\frac{d\tau_\nu(p)}{dx(p)}\,dx(p), \qquad (1)$$

where $R(\nu)$ is the outgoing spectral radiance within a spectral channel centered at frequency ν, B_ν, the Planck radiance for temperature $T(p)$ at pressure p, $\tau_\nu(p)$ the transmittance of the atmosphere above pressure p, and $x(p)$ is an arbitrary function of pressure.

In particular, the radiation received at frequency ν is the sum of all the radiance contributions from the earth's surface and from all individual levels in the atmosphere.

$$R(\nu_j) = \sum_{i=1}^{N} B[\nu_j, T(p_i)]\,w(\nu_j, p_i) \qquad (2)$$

with

$$w(\nu_j, p_i) = \varepsilon(\nu_j, p_i)\,\tau(\nu_j, \sigma_{p_i})$$

In (2) $B[\nu_j, T(p_i)]$ is the Planck radiance source for the i^{th} pressure level (p_i), having a temperature T, $\varepsilon(\nu_j, p_i)$ is the emissivity of the emitting medium at the pressure p_j for radiation of frequency ν_j, $\tau(\sigma_{p_i})$ is the transmissivity of the atmosphere above the i^{th} pressure level.

$B(\nu,T)$ is explicitly

$$B(\nu,T) = C_1\nu^3/[\exp(C_2\nu/T)-1] \qquad (3)$$

where C_1 and C_2 are the constants of the Planck function.

The term on the right of (2) is the sum of the component of radiance arising from the surface and all the radiation components originating in the atmosphere itself. These radiance contributions are weighted by the function $w(\nu_j, P_i)$. The weighting functions for TOVS instruments are illustrated in Fig. 2.

The problem is to determine the temperature of the N levels from radiance observations at say M discrete frequencies. However, because of the vertical width of the weighting functions, there is no unique solution; that is, many different temperature profiles will give rise to the same radiance measurements. Furthermore, the temperature profile solution tends to be unstable in the sense that small radiance measurement errors tend to produce disproportionately large errors of temperature.

In view of these difficulties many methods for solving the numerical problem have been proposed. In most of these, the solution is approximated in a linear form. The coefficients of the solution can be defined in several ways.

3.2. The Numerical Solution

Because of the known nature of the atmosphere, there is no need to determine the entire magnitude of T. One always has available a reasonable guess of the solution, for example, a climatological mean for a forecast profile. Hence, it is convenient to write equation (2) in terms of a deviation from an initial state, denoted by the zero subscript,

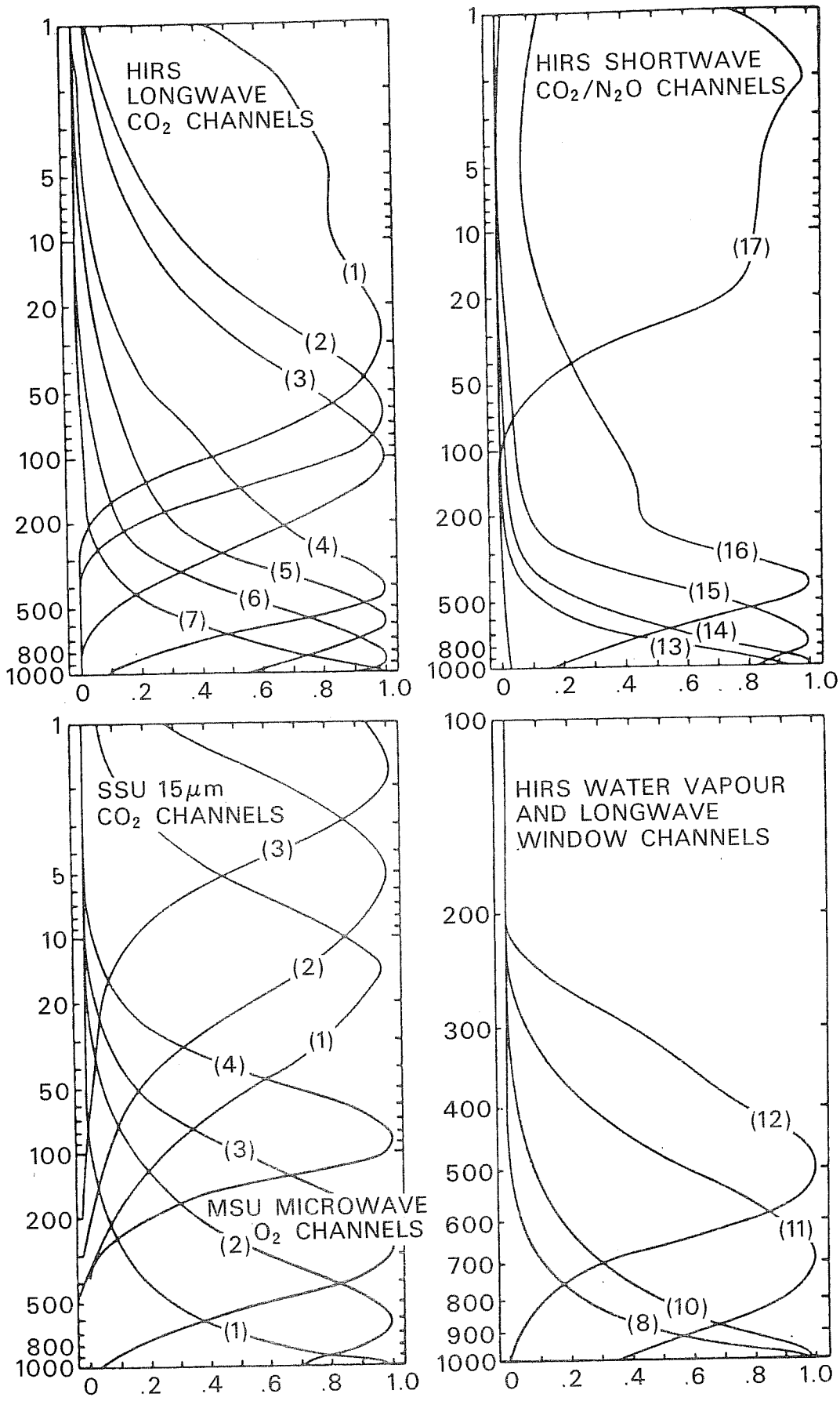

Fig. 2: TOVS weighting functions (normalized)

$$R(\nu_j)-R_o(\nu_j) = \sum_{i=1}^{N} B[\nu_j,T(P_i)]-B[\nu_j,T_o(P_i)] \quad W(\nu_j,P_i)+\varepsilon(\nu_j) \qquad (4a)$$

where $\varepsilon(\nu_j)$ is the measurement error. In matrix form

$$\underline{r} = \underline{\underline{b}}\underline{W} + \underline{\varepsilon} \qquad (4b)$$

In order to solve (4) for the temperature profile it is necessary to linearize the Planck function dependence upon frequency. This can be achieved since in the infrared region the Planck function is much more dependent upon temperature than frequency.

The general inverse solution (Fleming and Smith 1971) of (4) for the temperature profile takes the form

$$B[\nu_r,T(P_i)] - B[\nu_r,To(P_i)] = \sum_{i=1}^{M} a(\nu_j,P_i)[R(\nu_j)-R_o(\nu_j)] \qquad (5a)$$

where ν_r is the fixed central reference frequency used for the Planck function linearization and the temperature is obtained from the inverse of (3).

$$T = C_2\nu_r/\ln[(C_1\nu_r^3/B) + 1]. \qquad (5b)$$

The matrix form of (5) is

$$\underline{b} = \underline{r}\underline{\underline{A}} \tag{5c}$$

Assuming negligible measurement error, the coefficients $A(\gamma_j, p_i)$, that is

$$\underline{\underline{A}} = \underline{\underline{W}}^{-1} \tag{6}$$

where "-1" denotes the inverse matrix. In practice, however, "A" cannot be defined by (6) because of the near singularity of the matrix W. This is due to the lack of vertical independence of the weighting functions as can be seen in Fig. 2. This direct solution is highly unstable in the sense that small errors of radiance measurement cause disproportionately large errors of temperature.

3.2.1 Statistical Regression Solution

The statistical regression solution makes use of the large quantity of atmospheric temperature data provided by conventional means (e.g., from radiosondes and rocketsondes). If one has a sample of conventional measurements that are coincident in space and time with satellite measurements, the coefficient matrix "A" can be determined by standard linear regression techniques. The solution is

$$\underline{\underline{A}} = (\underline{\underline{R}}^T \underline{\underline{R}})^{-1} \underline{\underline{R}}^T \underline{\underline{B}} \tag{7}$$

where $(\underline{\underline{R}}^T \underline{\underline{R}})$ is the covariance of the measured spectral radiances and $(\underline{\underline{R}}^T \underline{\underline{B}})$ is the covariance of the measured radiances with atmospheric temperature.

In (7) the initial state is defined as the sample mean. Once "A" is determined from the sample of coincident observations, it can be used to obtain any particular solution using (5) and any arbitrary initial state (e.g., a forecast state). If actual measurements are used to determine "A", no explicit knowledge of the weighting functions is required. However, if the weighting functions are known the regression coefficients can be defined solely from conventional data. The coincident satellite measurements are simulated from the conventional data. Substituting (4) into (7) yields the solution

$$\underline{\underline{A}} = (\underline{\underline{W}}^T\underline{\underline{B}}^T\underline{\underline{B}}\underline{\underline{W}} + \underline{\underline{E}}^T\underline{\underline{E}})^{-1}\underline{\underline{W}}^T\underline{\underline{B}}^T\underline{\underline{B}} \qquad (8)$$

where B^TB is the covariance of atmospheric Planck radiance (temperature) and E^TE is the covariance of the random measurement errors which is determined from ground calibration data. The advantage of (8) is that the coefficients can be determined before satellite launch enabling the data processing to commence during the first day in orbit. Also a better statistical sample can be used since there is neither time nor space restrictions, in this formulation. The major limitations are caused by uncertainties in the weighting functions and any unknown bias measurement errors.

The current operational retrieval method is based on regressions, however, eigenvector of both radiance and temperature are used in order to improve the regression noise level (Smith and Woolf, (1976)).

3.2.2 Minimum Information Solution

A physical approximation of the regression relation (8), known as the "Minimum Information"-case (Smith, et al.(1972)) can be derived on the basis of two simplifying assumptions; (a) the temperature deviations from the initial state (or guess) are uncorrelated and their variance is a constant, σ_b^2, with respect to pressure level, and (b) the measurement errors are uncorrelated and their variance is a constant σ_ε^2, with respect to observation frequency.

Under these assumptions

$$\underline{\underline{B}}^T\underline{\underline{B}} = \sigma_b^2 I \qquad (9a)$$

and

$$\underline{\underline{E}}^T\underline{\underline{E}} = \sigma_\varepsilon^2 I \qquad (9b)$$

where I is the identity matrix. Substituting (8) into (7) yields the solution

$$\underline{\underline{A}} = (\underline{\underline{W}}^T\underline{\underline{W}} + \gamma \underline{\underline{I}})^{-1}\underline{\underline{W}}^T \qquad (10)$$

for

$$\gamma = \sigma_\varepsilon^2/\sigma_b^2$$

The minimum information solution (10) can be obtained solely from the weighting functions and an estimation of the variances of atmospheric temperature and radiance measurement error. It is essentially independent of a priori statistical data.

Although the loss of this statistical information must have an affect on the solution, the minimum information case permits temperature profiles to be obtained which maintains small vertical scale structure in a forecast guess.

The comparative study to follow was conducted to illustrate the similarities and differences of the statistical regression and minimum information solutions.

3.3. The Comparative Study

Four hundred sets of SIRS-A radiance measurements and conventional temperature soundings were used to generate regression coefficients for the thirteen standard pressure levels (i.e., 1000, 850, 700, 500, 400, 300, 250, 200, 150, 100, 50, 30, 10 mb levels). The statistical sample, was restricted to the months of August and September, 1969. The radiances were corrected for the effects of clouds using the procedure of Smith, Woolf, and Jacob (1970). Fig. 4 shows the regression coefficients obtained.

As may be seen the levels of the maximum positive values generally correspond with the levels where the weighting functions are a maximum (Fig. 3). The negative valued coefficients are a result of the vertical interdependence of the various spectral radiance observations.

Coefficients were also determined for the minimum information case using weighting functions calculated from the mean profile of the above statistical sample. These minimum information coefficients are illustrated in Fig. 5. The general shapes and levels of maximum value closely resemble those obtained through statistical regression. This resemblance indicates

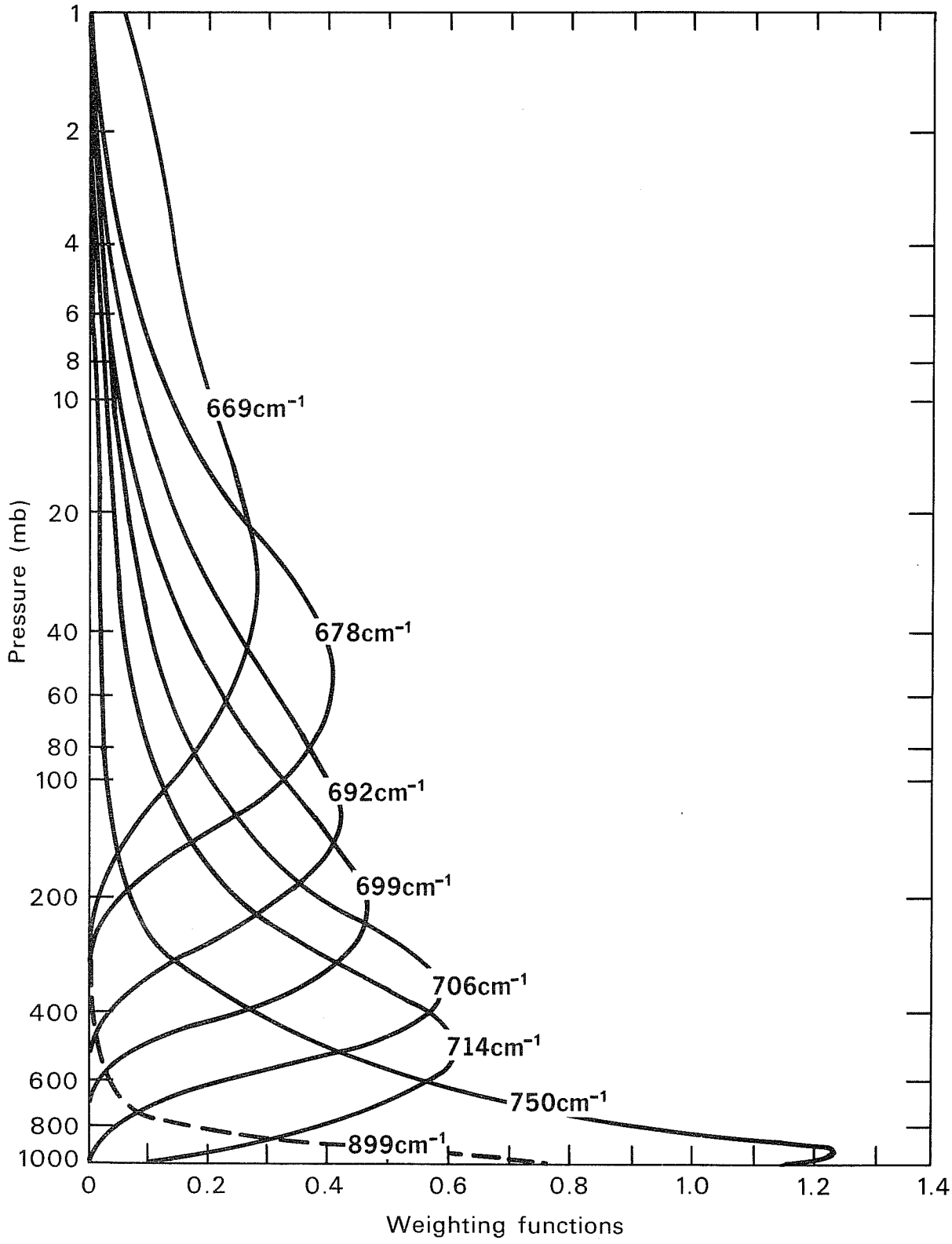

Fig. 3: SIRS-A weighting functions

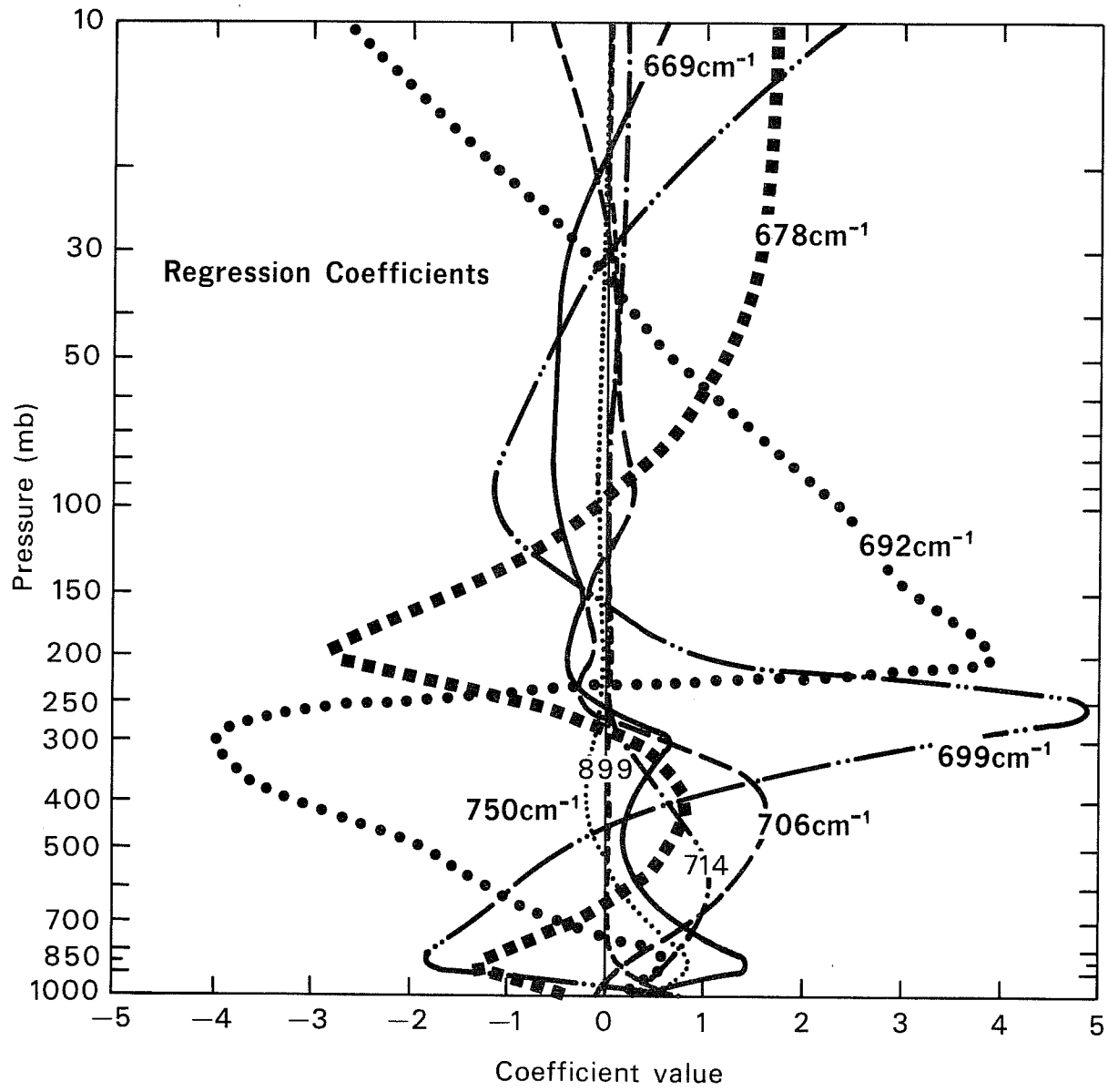

Fig. 4: Regression solution coefficients

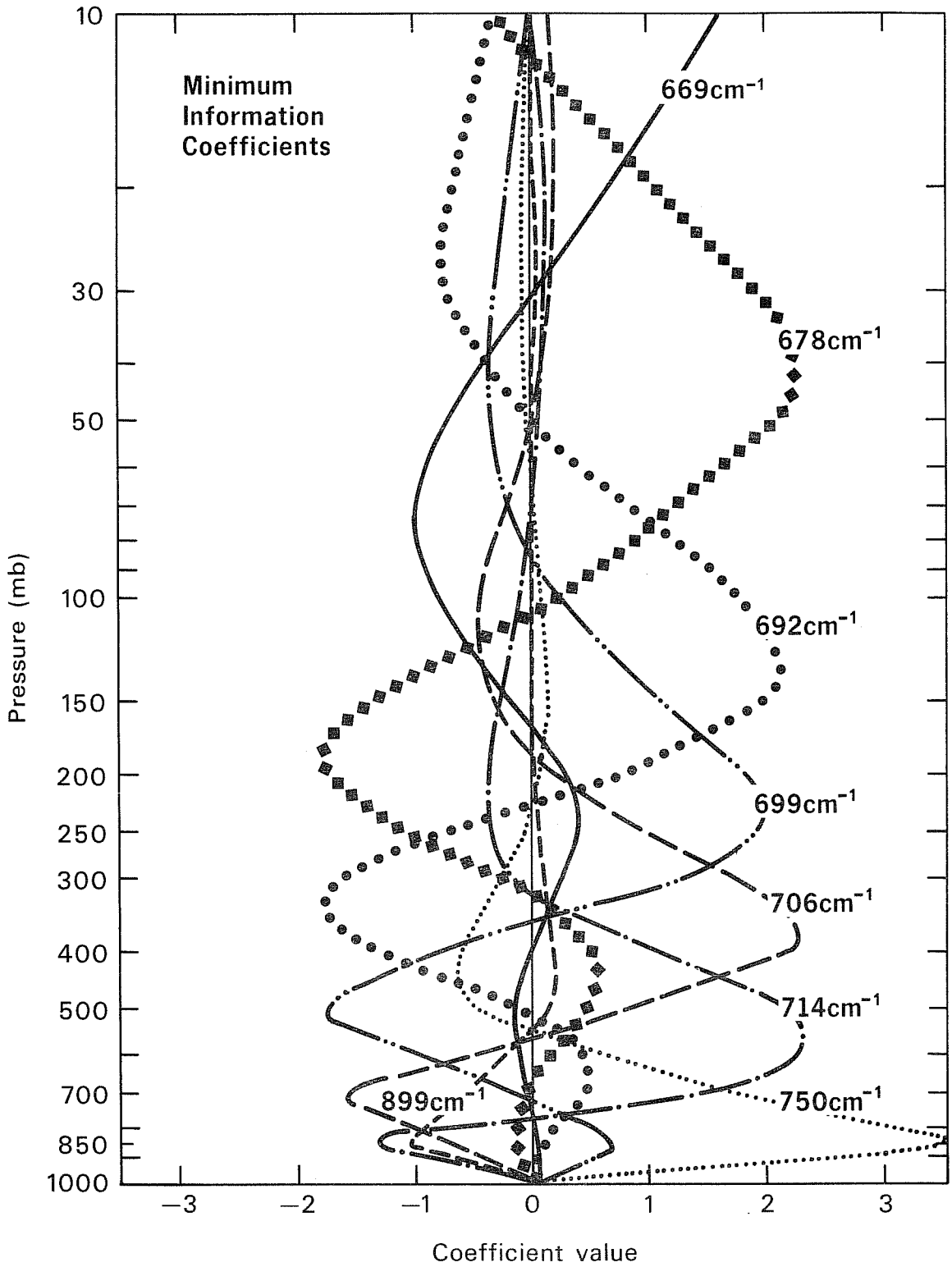

Fig. 5: Minimum information solution coefficients

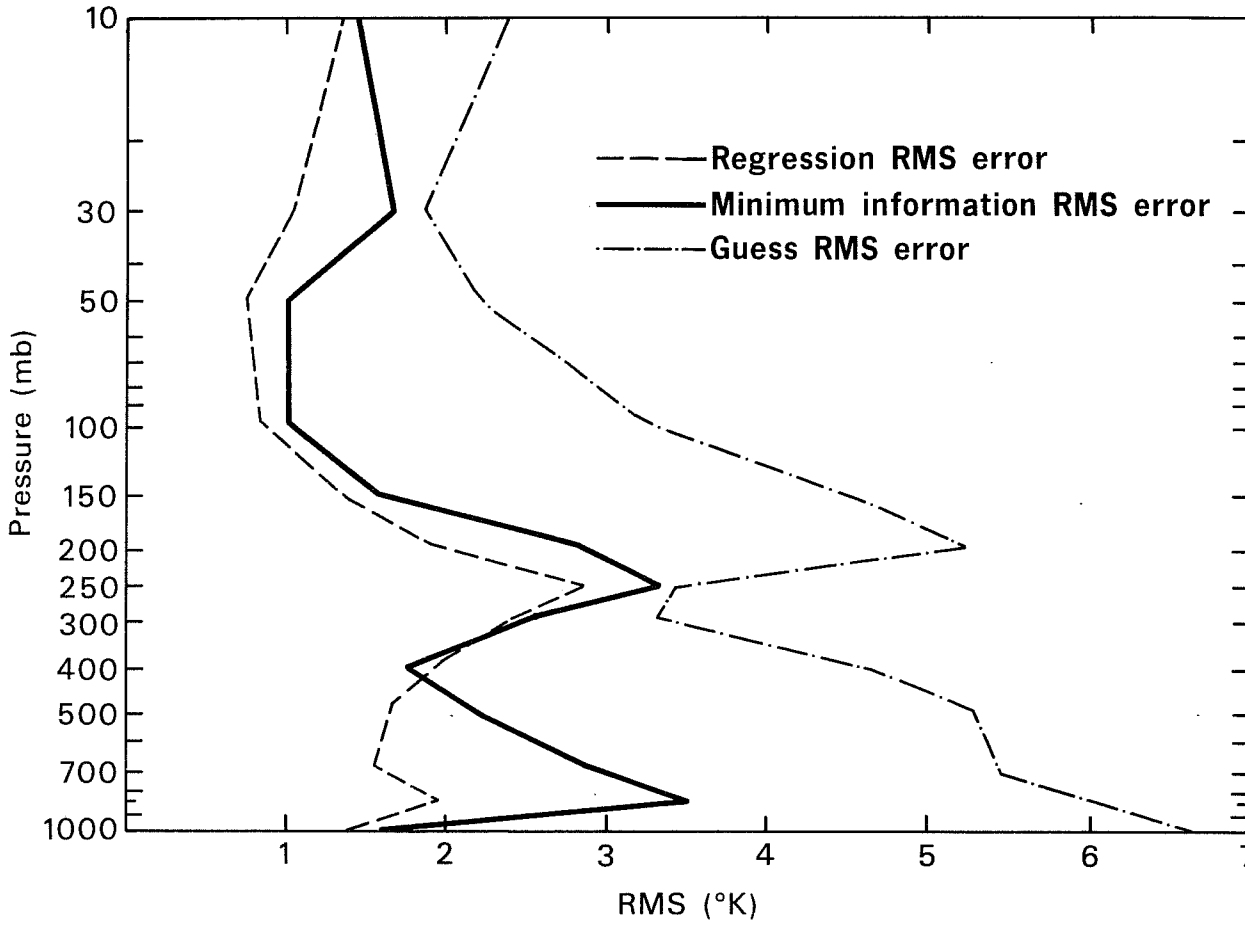

Fig. 6: Comparison of RMS error distributions

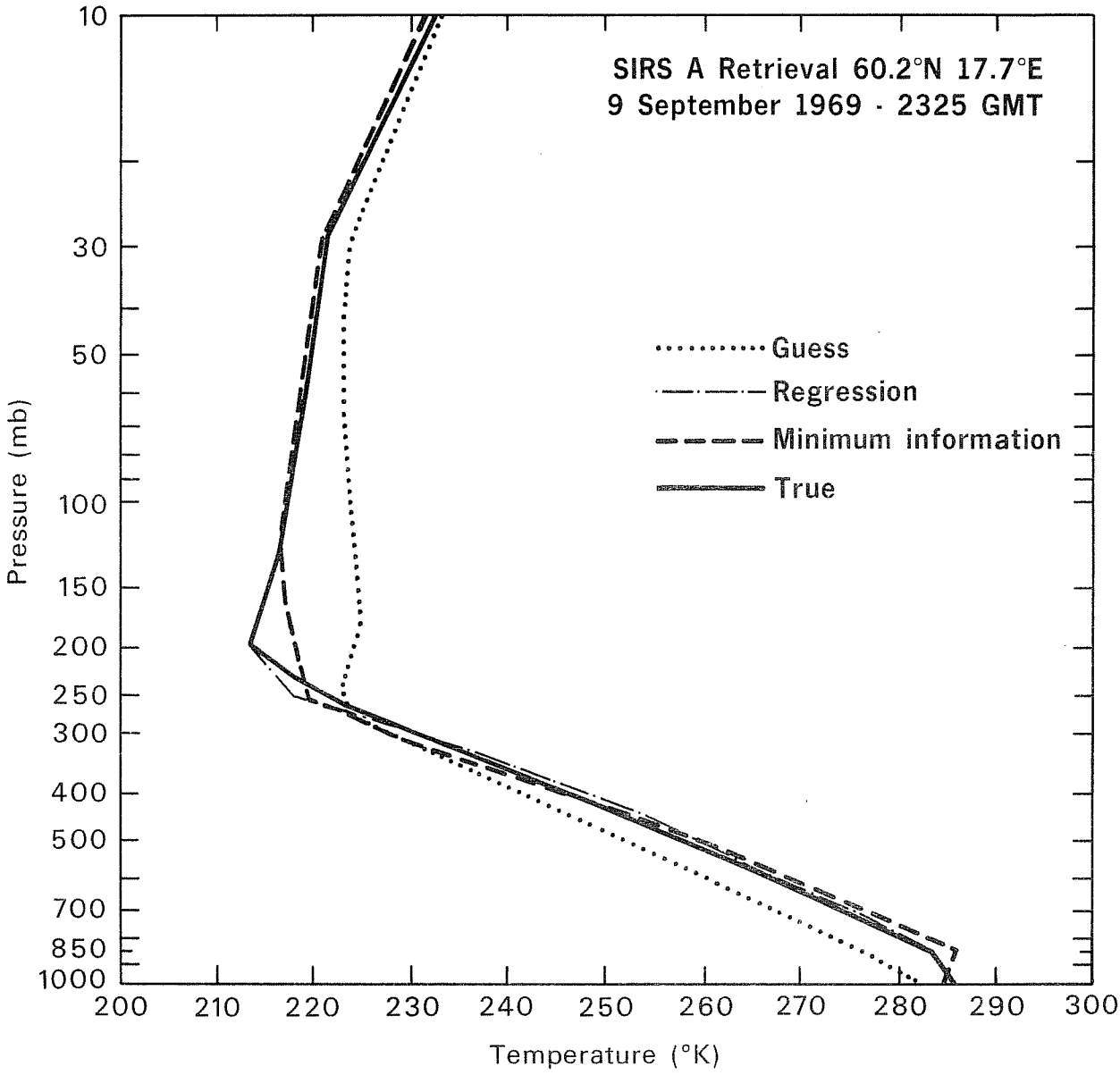

Fig. 7: Comparison between SIRS-A derived temperature profiles and a conventional RAOB (True)

that the regression coefficients are mainly dependent upon the weighting functions and not on the covariances of atmospheric temperature. Significant differences, however, occur in the tropopause region (100-300 mb) and near the earth's surface.

Both sets of coefficients were then used to calculate temperature profiles from a statistically independent set of 120 cloudless radiance observations obtained during September, 1969. In both cases the mean profile of the regression sample was used as the initial guess. Corresponding radiosonde observations were used to verify the two solutions.

Fig. 6 displays the RMS temperature error associated with the two solutions along with the RMS error of the initial guess. The largest errors are seen at the tropopause and near the surface.

The tropopause and surface inversion are difficult to retrieve due to the relatively poor vertical resolution provided by the weighting functions. It can be seen that statistics help to overcome the vertical resolution related deficiencies, especially near the earth's surface. In other regions of the atmosphere, the middle troposphere and the lower stratosphere, there is only minor improvement using actual statistical relationships.

Fig. 7 shows a temperature profile retrieval which depicts the solution characteristics noted above.

The regression and minimum information solutions are both satisfactory throughout the middle troposphere and lower stratosphere. The minimum information solution however failed to capture the radiosonde observed tropopause characteristic. This feature was recoverable from the radiance observations using statistical regression relations.

4. COMPARISON OF TOVS AND RADIOSONDE TEMPERATURES AND PRECIPITABLE WATER MEASUREMENTS

There have been a number of comparisons made (Phillips et al.(1979), Gruber and Watkins (1981, 1982), McMillin et al.(1983)) and most recently Johnson (1984) and only a brief summary will be presented.

There have been three major changes to the operational global processing at Washington since the end of the FGGE observational year. Two modifications to the microwave processing have helped eliminate heavy rainfall effects and improve oceanic microwave temperature retrievals. Also the processing of partly cloudy radiances to deriving 'clear columns' has been improved (McMillin and Dean (1982)).

Table 2, based on McMillin et al.(1983), shows some improvement between 1979-80 and 1981-82. Table 3, produced by Phillips, (see Johnson (1984)), also shows improved accuracy for oceanic soundings after FGGE.

It is important to consider how representative these above comparisons are when there are errors in the radiosondes and also errors due to space and time mislocation. McMillin has attempted to convect for the space and time error and the results are shown in Table 4. There is considerable improvement using a space/time correction. This is more fully discussed by Johnson (1984). In general there has been a small improvement with each new modification to the operational processing, however, the sounding errors are now close to their theoretical estimates and the limitation is due to the broad weighting functions.

Table 2

Yearly* Average RMS Differences between Satellite Soundings and Radiosondes

(Based on McMillin et al., 1983)

* 1 November-31 October

Layer (mb)	Clear		Partly Cloudy		Cloudy	
	1979-80	1981-82	1979-80	1981-82	1979-80	1981-82
1000-850	2.81	2.88	3.10	3.03	3.78	3.62
850-700	2.35	2.32	2.73	2.63	3.36	3.20
700-500	2.02	1.95	2.14	2.03	2.74	2.54
500-400	2.31	2.21	2.41	2.32	2.96	2.78
400-300	2.28	2.16	2.37	2.31	2.97	2.65
300-200	2.29	2.14	2.47	2.15	2.83	2.46
200-100	2.07	1.97	2.19	1.99	2.33	2.22
100- 70	2.16	2.02	2.16	2.08	2.24	2.14

Comparisons calculated from radiosondes within $\pm$3 hours and 3 degrees of latitude from the satellite observation.

Table 3

RMS Differences Between Satellite Soundings and Radiosondes

30 - 60°N

(Based on Phillips et al., 1979 and Phillips, private communication)

	30 JAN-28 FEB 79		29 MAR-27 APR 79		17-30 NOV 1981	
Layer (mb)	Mostly Clear	Mostly Cloudy	Mostly Clear	Mostly Cloudy	Partly Cloudy	Mostly Cloudy
1000-850	2.9	4.0	2.3	3.1	2.7	2.4
850-700	2.1	3.1	1.4	2.4	2.2	2.3
700-500	2.6	3.3	1.7	2.4	1.6	1.5
500-400	2.2	3.3	1.8	2.5	2.0	2.2
400-300	2.2	3.1	2.2	2.4	2.2	2.4
300-200	2.2	2.8	2.0	1.9	2.0	1.9
200-100	1.8	1.6	1.8	1.6	1.5	1.5

- Only ocean colocations are used.
- Radiosondes are interpolated in time to that of the satellite soundings and the satellite soundings are interpolated to the radiosonde locations.
- TIROS-N only in 1979, both TIROS-N and NOAA-6 included in 1981.

Table 4

Comparison of Interpolation and Non-interpolation Techniques for Calculating RMS Differences Between Satellite Soundings and Radiosondes

(Based on McMillin et al., 1983)

Layer (mb)	Interpolated(1)	Non-interpolated(2)
1000-850	2.1	2.7
850-700	1.7	2.2
700-500	1.2	1.8
500-300	1.3	2.1
300-200	2.0	2.0
200-100	2.0	1.9
100- 70	1.4	1.7
70- 50	1.3	1.9
50- 30	1.3	1.8
30- 10	1.9	2.4

(1) The method of Phillips et al. (1979) in which 12h radiosondes are interpolated in time to that of the satellite soundings, and the satellite soundings within 600km of the radiosonde location are interpolated to that location.

(2) Colocations within $\pm$3h and 3 degrees of latitude taken as an exact colocation in space and time.

Table 5

Comparisons of Precipitable Water Measured by TIROS-N and Radiosondes, Eastern United States

16-18 April 1979 (58 samples)

Precipitable water (cm)

Layer	TIROS-N Mean	TIROS-N Std Dev	Radiosonde Mean	Radiosonde Std Dev	Difference* Mean	Difference* Std Dev
Sfc-700	1.2	0.3	0.9	0.4	0.3	0.5
700-500	0.3	0.1	0.2	0.1	0.1	0.1
Total	1.6	0.4	1.2	0.5	0.4	0.6

8-11 September 1979 (106 samples)

Sfc-700	2.1	0.6	2.0	0.9	0.1	0.5
700-500	0.6	0.2	0.5	0.3	0.1	0.2
Total	2.9	0.8	2.6	1.1	0.3	0.6

* The means and standard deviations of the individual comparisons, TIROS-N minus radiosonde.

There are problems associated with obtaining vertical profiles of moisture, particularly near the surface. This is discussed in more detail by Johnson (1984). Table 5 shows results obtained by Gruber and Watkins (1981). The major problem is the water vapour structure is very complex and statistical relations between satellite radiance and radiosonde measurements are much poorer than temperature. The other major limitation is cloud, in particular, small clouds which partly fill the field of view of the HIRS sensor and are not accounted in the clear radiance calculations.

5. CONCLUSIONS

The operational TOVS package is producing radiosonde like profiles close to their theoretical accuracy and these profiles have been transmitted at 500 km resolution via the GTS since FGGE. In the past few months their resolution has been improved (250 km) with the addition of a new code proposed and implemented by ECMWF and NMC in Washington. It is now becoming clear that there is far more information in the horizontal than is presently being transmitted and that the satellite measurements only contain perhaps five or six pieces of information in the vertical. There is an important need to develope new methods of using these data in numerical analyses.

REFERENCES

Fleming, H. E. and Smith, W.L., 1971, Inversion Techniques for Remote Sensing of Atmospheric Temperature Profiles, Proceeding of the Fifth Symposium on Temperature, Its Measurement and Control in Science and Industry, Washington, D. C.

Gruber, A., and Watkins, C. D., 1981, Preliminary evaluation of initial atmospheric moisture from the TIROS-N sounding system. In Satellite Hydrology (Deutsch, M., Wiesnet, D. R., and Rango, A., eds.), Amer. Water Res. Assn., Minneapolis, Minn., 115-123.

Gruber, A., and Watkins, C. D., 1982, Statistical assessment of the quality of TIROS-N and NOAA-6 satellite soundings. Mon. Wea. Rev., 110, 867-876.

Johnson, D. S., 1984, Meteorological parameters derived from space-based observing systems - FGGE and after ECMWF Seminar on Data Assimilation systems and observing system experiment with particular emphasis on FGGE, 3-7 September 1984.

McMillin, L., and Dean, C., 1982, Evaluation of a new operational technique for producing clear radiances. J. Appl. Meteorolog., 21, 1005-1014.

McMillin, L., Gray, D. G., Drahos, H. F., Chalfant M. W., and Novak, C. S., 1983, Improvements in the accuracy of operational satellite soundings. J. Clim. and Appl. Meteorol., 22, 1948-1955.

Phillips, N. A., McMillin, L., Gruber, A., and Wark, D., 1979, An evaluation of early operational temperature soundings from TIROS-N. Bull. Am. Meteorol. Soc., 60, 1188-1197.

Smith, W. L., Woolf, H. M., and Jacob, W. J., 1970, A Regression Method for Obtaining Real Time Temperature and Geopotential Height Profiles from Satellite Spectrometer Measurements and Its Application to Nimbus III 'SIRS' Observations, Mon. Wea. Rev., 98, 582-603.

Smith, W. L., Woolf, H. M., and Fleming, H. E., 1972, Retrieval of Atmospheric Temperature Profiles from Satellite Measurements for Dynamical Forecasting, J. Applied Meteor., 11, No. 1.

Smith, W. L., and Woolf, H. M., 1976, The use of eigenvectors of statistical covariance matricies for interpreting satellite sounding radiometer observations. J. Atmos. Sci., 33, 1127-1140.

Smith, W.L., Woolf, H. M., Hayden, C. M., Wark, D. Q., and McMillin, L. M., 1979, The TIROS-N Operational vertical sounder. Bull. Am Meteorol. Soc., 60, 1177-1187.